N92-22190

A Finite Element Formulation for Scattering from Electrically Large 2-Dimensional Structures.

Daniel C. Ross and John L. Volakis

January 5, 1992

Abstract—A Finite Element Formulation is given using the scattered field approach with a fictitious material absorber to truncate the mesh. The formulation includes the use of arbitrary approximation functions so that more accurate results can be achieved without any modification to the software. Additionally, non-polynomial approximation functions can be used, including complex approximation functions. The banded system that results is solved with an efficient sparse/banded iterative scheme and as a consequence, large structures can be analyzed. Results are given for simple cases to verify the formulation and also for large, complex geometries.

I. Introduction

The popularity of the Finite Element Method (FEM) in Electromagnetic Scattering is largely due to the fact that the method results in a banded system with an $O(N)$ memory demand. This is in sharp contrast to the Moment Method which has an $O(N^2)$ memory demand. For open region scattering problems however, the Finite Element region must be artificially truncated in order to bound the problem. This has been accomplished with approximate methods such as the Uni-Moment Method [1] and the Absorbing Boundary Condition [6] and more successfully with the rigorous Boundary Integral Technique [3]. Unfortunately, the solution of the Boundary Integral in general results in a dense system thus destroying the $O(N)$ character of the FEM. Also, the boundary integral technique breaks down at resonant frequencies and these resonant frequencies become more and more closely spaced as the size of the boundary is increased.

More recently, the technique of using a fictitious material absorber to confine the scattered field has been suggested in [4]. Since fictitious materials having a negative real part of μ and ϵ can be used, an absorber with a very low reflection coefficient even at near grazing incidence can be realized. Also, this technique requires the unknown quantity to be the scattered field, not the total field as is usually the case. The benefits of this are two-fold. First, the scattered field does not vary as rapidly as the total field and second, the scattered field approach requires that the incident field be evaluated in the interior of the mesh, thus reducing the phase error
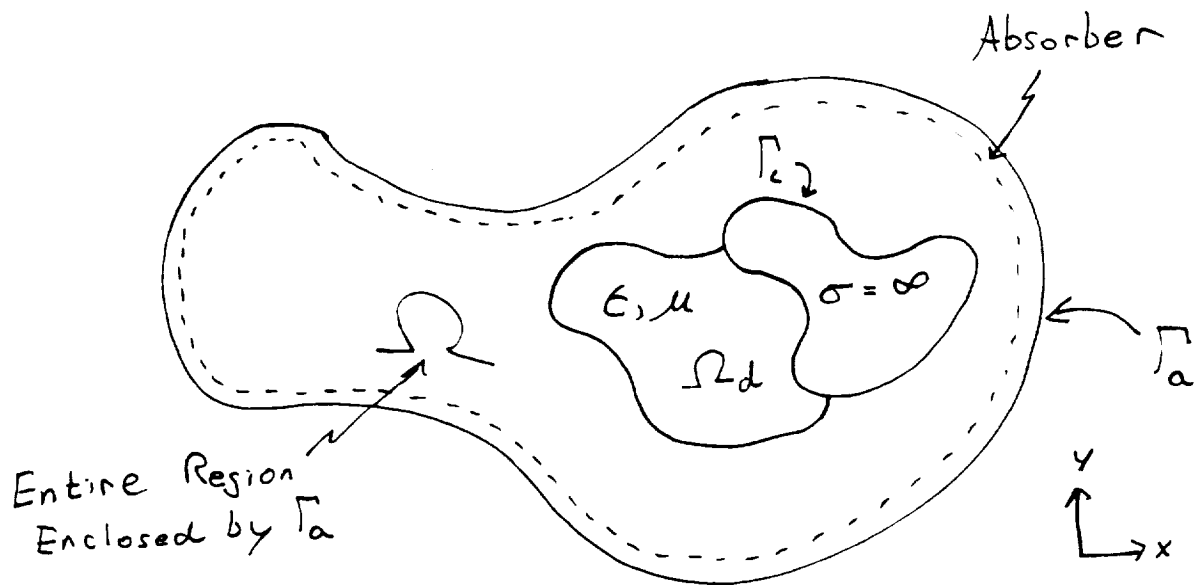
1

Figure 1: Region of solution

normally associated with the total field approach. That is, the total field approach requires that the incident field be evaluated only at the fictitious boundary and then propagate through the mesh to the scatterer thus introducing phase error, especially notable when the mesh is large. It has been confirmed in [5] that the scattered field approach results in a more accurate solution.

It is known that there is also an overall inherent error in the FEM that does not exist in the Moment Method [7]. This error is a result of the bandedness of the system and is introduced as the solution propagates through the mesh. In fact, experience has shown that as the mesh area increases, the element size must decrease. The only solution to this problem is to use higher order approximation functions, which usually involves a complete re-formulation and re-design of the software.

In this paper a number of advances in FEM calculations are combined to give a solution to the 2-Dimensional Helmholtz equation for electrically large scatterers. The scattered field approach is used and a fictitious material absorber is used to truncate the mesh. Unique to this formulation is the use of arbitrary approximation functions that make it possible to increase the accuracy of the solution without modifying the software.

II. Formulation

Consider the region shown in Figure 1.

Given that there is some incident field, we wish to solve the wave equation in the region Ω and find the fields scattered by the dielectric/magnetic/conducting target.

The source free wave equation in two dimensions can be written

$$\nabla \cdot (u\nabla\phi) + k_0^2 v\phi = 0 \tag{1}$$

where

$$\phi = E_z \tag{2}$$

$$u = 1/\mu_r \tag{3}$$

$$v = 1/\epsilon_r \tag{4}$$

for E polarization (z directed electric field)

and

$$\phi = H_z \tag{5}$$

$$u = 1/\epsilon_r \tag{6}$$

$$v = 1/\mu_r \tag{7}$$

for H polarization (z directed magnetic field)

Now let T be some compactly supported testing function used to enforce (1) over the entire region.

$$\iint_\Omega T[\nabla \cdot (u\nabla\phi) + k_0^2 v\phi]\, ds = 0 \tag{8}$$

Using the identity

$$T[\nabla \cdot (u\nabla\phi)] = -u(\nabla\phi \cdot \nabla T) + \nabla \cdot (Tu\nabla\phi) \tag{9}$$

gives

$$\iint_\Omega [u(\nabla T \cdot \nabla\phi) - k_0^2 v T\phi]\, ds - \iint_\Omega \nabla \cdot (Tu\nabla\phi)\, ds = 0 \tag{10}$$

and applying the divergence theorem to the second term in the above brings us to the weak form of eqn. (1).

$$\iint_\Omega [u(\nabla T \cdot \nabla\phi) - k_0^2 v T\phi]\, ds - \oint_{\Gamma_a} uT\frac{\partial\phi}{\partial n}\, d\ell - \oint_{\Gamma_c} uT\frac{\partial\phi}{\partial n}\, d\ell = 0 \tag{11}$$

To use eqn. (11) in an FEM implementation would be considered a total field approach since the unknowns would be the total field. To get the analog of (11) with the scattered field as the unknown we let

$$\phi = \phi^s + \phi^i \tag{12}$$

3

and (11) becomes

$$\iint_\Omega [u(\nabla T \cdot \nabla \phi^s) - k_0^2 v T \phi^s]\, ds - \oint_{\Gamma_a} T(u\frac{\partial \phi^s}{\partial n} + \tilde{u}\frac{\partial \phi^i}{\partial n})\, d\ell \tag{13}$$

$$- \oint_{\Gamma_c} T(u\frac{\partial \phi^s}{\partial n} + \tilde{u}\frac{\partial \phi^i}{\partial n})\, d\ell = - \iint_\Omega [\tilde{u}(\nabla T \cdot \nabla \phi^i) - k_0^2 \tilde{v} T \phi^i]\, ds$$

where $\tilde{u}$ and $\tilde{v}$ are the material constants of the scatterer in a free space environment while u and v include the fictitious absorber. In this way the incident field does not interact with the fictitious absorber.

In either case, eqns. (11) and (13) require that the normal derivative of the unknown (total field and scattered field respectively) be specified on the enclosing boundaries Γ_a and Γ_c. These normal derivatives are arbitrary, and once given, a solution in the interior is uniquely defined.

For E polarization we will put a perfect magnetic conductor at Γ_a and for H polarization we will put a perfect electric conductor at Γ_a thus the second term on the LHS of (13) is

$$- \oint_{\Gamma_a} \tilde{u} T \frac{\partial \phi^i}{\partial n}\, d\ell \tag{14}$$

Note that this conductor is seen by the scattered field only, not the total field.

The boundary condition at Γ_c is

$$\frac{\partial \phi^s}{\partial n} + \frac{\partial \phi^i}{\partial n} = 0 \tag{15}$$

for H polarization, and thus the third term on the LHS of (13) is zero.

For E polarization the boundary condition at Γ_c is

$$\phi^s + \phi^i = 0 \tag{16}$$

and since the solution is specified on this contour, the normal derivatives will uncouple from the rest of the equation once we have discritized (13) and created a linear system, thus the third term on the LHS of (13) drops out.

We have that eqn. (13) becomes

$$\iint_\Omega [1/\mu_r(\nabla T \cdot \nabla \phi^s) - k_0^2 \epsilon_r T \phi^s]\, ds - \oint_{\Gamma_a} 1/\tilde{\mu}_r T \frac{\partial \phi^i}{\partial n}\, d\ell = \tag{17}$$

$$- \iint_\Omega [1/\tilde{\mu}_r(\nabla T \cdot \nabla \phi^i) - k_0^2 \tilde{\epsilon}_r T \phi^i]\, ds$$

for E polarization and

$$\iint_\Omega [1/\epsilon_r(\nabla T \cdot \nabla \phi^s) - k_0^2 \mu_r T \phi^s]\, ds - \oint_{\Gamma_a} 1/\tilde{\epsilon}_r T \frac{\partial \phi^i}{\partial n}\, d\ell = \tag{18}$$

$$- \iint_\Omega [1/\tilde{\epsilon}_r(\nabla T \cdot \nabla \phi^i) - k_0^2 \tilde{\mu}_r T \phi^i]\, ds$$

4

for H polarization.

The region Ω now is divided into arbitrary, polygonal finite elements. Each element is defined by its corner nodes and may contain other nodes located anywhere in the element. The solution in the e'th element is approximated by

$$\phi^e(x,y) = \sum_{n=1}^{N^e} S_n^e(x,y)\phi_n^e \qquad (19)$$

where N^e is the total number of nodes in the e'th element, ϕ_n^e is the value of ϕ at the n'th node and $S_n^e(x,y)$ is the n'th shape function for the e'th element understood to be zero outside of the e'th element. These shape functions will be defined in the next section. To solve (17) and (18) using Galerkin's method, we let the testing function T be the same as the basis function in (19).

Substituting (19) into (17) and (18) gives the Element Equations

$$\iint_{\Omega_e} [1/\mu_r^e \nabla S_i^e \cdot \nabla \sum_{j=1}^{N^e} S_j^e \phi_j^e - k_0^2 \epsilon_r^e S_i^e \sum_{j=1}^{N^e} S_j^e \phi_j^e]\, ds = \qquad (20)$$

$$+ \oint_{\Gamma_a} 1/\tilde{\mu}_r^e S_i^e \frac{\partial \phi^i}{\partial n}\, d\ell - \iint_{\Omega_e} [1/\tilde{\mu}_r^e(\nabla S_i^e \cdot \nabla \phi^i) - k_0^2 \tilde{\epsilon}_r^e S_i^e \phi^i]\, ds \quad i = 1,2,3...N$$

for E polarization and

$$\iint_{\Omega_e} [1/\epsilon_r^e \nabla S_i^e \cdot \nabla \sum_{j=1}^{N^e} S_j^e \phi_j^e - k_0^2 \mu_r^e S_i^e \sum_{j=1}^{N^e} S_j^e \phi_j^e]\, ds = \qquad (21)$$

$$+ \oint_{\Gamma_a} 1/\tilde{\epsilon}_r^e S_i^e \frac{\partial \phi^i}{\partial n}\, d\ell - \iint_{\Omega_e} [1/\tilde{\epsilon}_r^e(\nabla S_i^e \cdot \nabla \phi^i) - k_0^2 \tilde{\mu}_r^e S_i^e \phi^i]\, ds \quad i = 1,2,3...N$$

for H polarization.

Again, $\tilde{\mu}_r^e$ and $\tilde{\epsilon}_r^e$ are the material constants of the scatterer in a free space environment while μ_r^e and ϵ_r^e include the fictitious absorber.

Equations (20) and (21) define an N^e by N^e linear system for a single element. Assembling all of the element systems together and converting to global node numbers gives the global finite element system

$$[K]\{\phi^s\} = \{\Phi^i\} \qquad (22)$$

For E polarization only, the boundary condition (16) must be enforced by setting $\phi^s = -\phi^i$ for nodes on the conductor.

III. Arbitrary Approximation Functions

5

In eqn. (19) the expansion of the solution was given as a sum of N shape functions weighted by the nodal values of the solution. To determine these shape functions let

$$\phi^e(x,y) = \sum_{n=1}^{N^*} a_n f_n(x,y) \qquad (23)$$

where the $f_n(x,y)$'s are linearly independent functions known as approximation functions.

Forcing $\phi^e(x,y)$ to be $\phi_i^e(x_i,y_i)$ at each nodal point gives the system

$$[F_{ij}^e]\{a_i^e\} = \{\phi_i^e\} \qquad (24)$$

where $[F_{ij}^e]$ is an N by N matrix whose i,j'th element is given by $f_j(x_i,y_i)$ and x_i,y_i are the coordinates of the i'th node. For ease of programming, these approximation functions are often chosen to be linear, ie. $f_1 = 1, f_2 = x, f_3 = y$. However, since it is known that higher order approximation functions result in better conditioned systems and are more accurate[1], it is desirable to use approximation functions of arbitrary order or even of a non-standard type such as complex transcendental functions which are better suited for Electromagnetics.

The shape functions are then given by

$$S_n^e(x,y) = \sum_{i=1}^{N^*} f_i(x,y)[F_{in}^e]^{-1} \qquad (25)$$

Notice that the first derivatives of the shape functions are also required and this must be taken into account when choosing approximation functions since from (23), derivatives of the shape function transfer directly to the approximation functions.

Note also that the inverse of an N^e by N^e matrix is required to calculate the shape function for each element. Since N^e will not be very large, this does not introduce any great expense.

When the arbitrary shape functions are used to generate the element matrices an efficient numerical integration scheme must be used. Since the elements are arbitrary polygons, an integration algorithm based on the polygon fill algorithm from computer graphics was developed. This integration algorithm takes as input: the number of points defining the polygon, the coordinates of these points, the number of sub-regions to split the area into, the order of the Gaussian quadrature to use, and the integrand function. With some experimentation, it was found that increasing the accuracy of the integrations had little effect on the far field scattering patterns once the integrations were approximately five percent accurate (for linear shape functions.)

IV. Results

The bistatic RCS pattern for a perfectly conducting circular cylinder of radius $\lambda/2$ is shown in figure 2. Linear shape functions were used and as can be seen from figure 3 a discretization of $\lambda/20$ was required. The fictitious absorber was placed $\lambda/2$ away from the cylinder to avoid interactions with the scatterer.
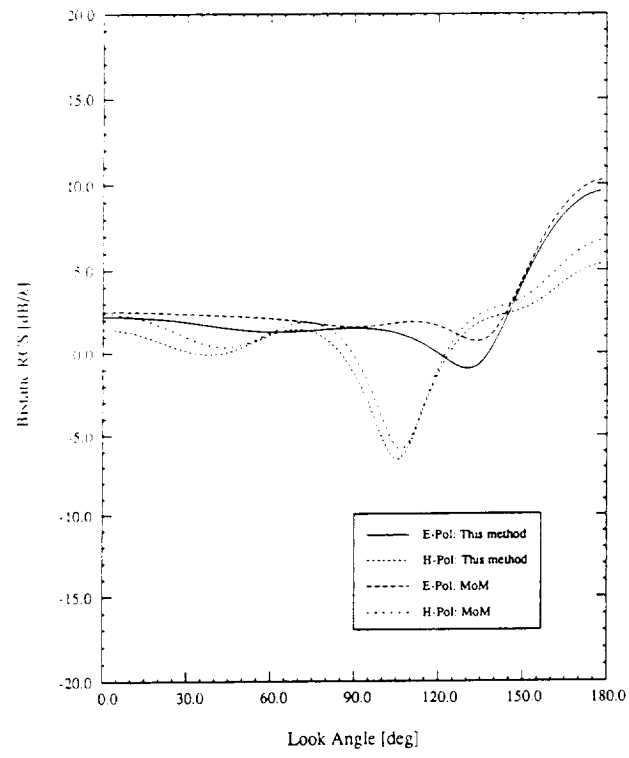
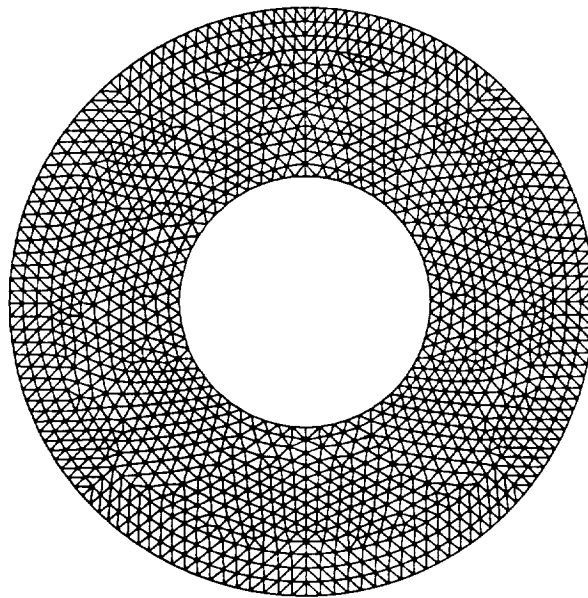Figure 2: Bistatic RCS of conducting cylinder

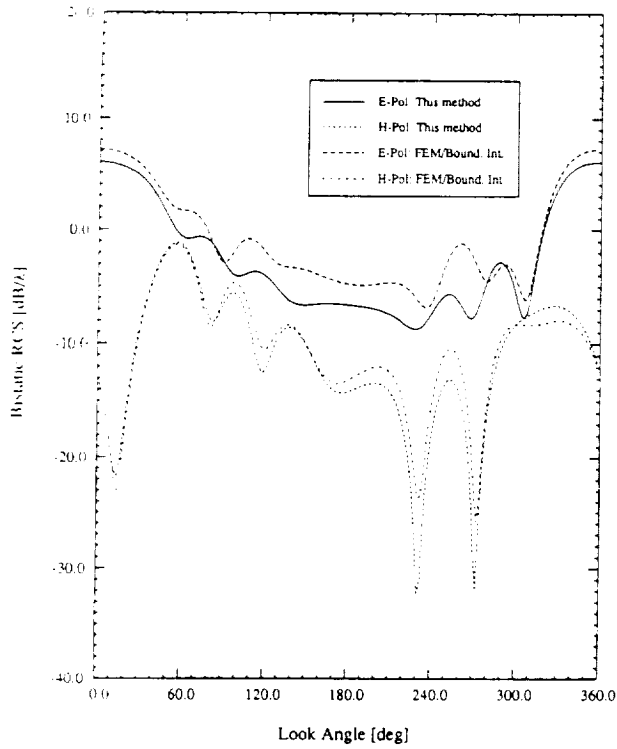Figure 3: Mesh for $r = \lambda/2$ conducting cylinder

7

Figure 4: Bistatic RCS of Airfoil

A more useful result is shown in figure 4 for a perfectly conducting airfoil at low frequency. The wing is approximately $1\frac{3}{4}\lambda$ long and as can be seen from figure 5 a discretization of $\lambda/20$ was again required but the fictitious absorber needed to be placed a full wavelength away from the target in order to get accurate results for H polarization. The reason for the discrepancy in the E polarization results is that the artificial absorber actually needs to be placed farther away from the scatterer. The following discussion addresses this issue.

For quadratic shape functions, which are obtained by setting $f_1 = 1, f_2 = x, f_3 = y, f_4 = xy, f_5 = x^2$, and $f_6 = y^2$, the mesh is not as dense as can be seen from figure 6. However since there are twice as many nodes per element, the net effect is that there are about half as many elements but the same number of nodes. However the increase in accuracy makes it possible to analyze larger and more detailed scatterers.

For cubic shape functions, which are obtained by setting, for example, $f_1 = 1, f_2 = x, f_3 = y, f_4 = xy, f_5 = x^2, f_6 = y^2, f_7 = x^3, f_8 = y^3, f_6 = x^3y^3$, the mesh is even less dense as can be seen from figure 7. Again, there are approximately the same number of nodes but the number of elements is cut in half. Actually, since the accuracy is increased exponentially, the mesh size could be increased further thus actually reducing the number of unknowns. This would seem to imply that higher order approximation functions keep getting more efficient. Whether or not this is the case remains to be seen.

Another choice of approximation function could be the Hankel function of order 0. This would make it possible to discretize using larger elements far away from the scatterer where the wave becomes somewhat cylinderical. There would still be other approximation functions to allow

---

[1]Polynomial approximation functions of Order p result in a solution which is h^p accurate where h is the mesh size.
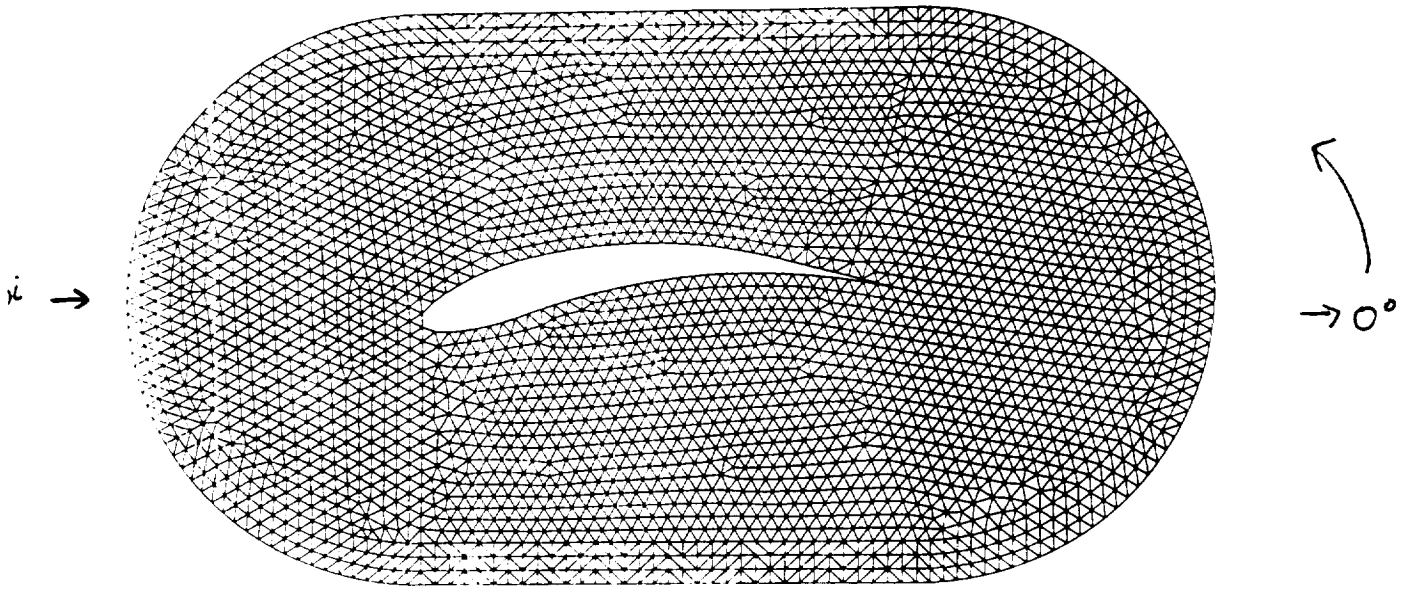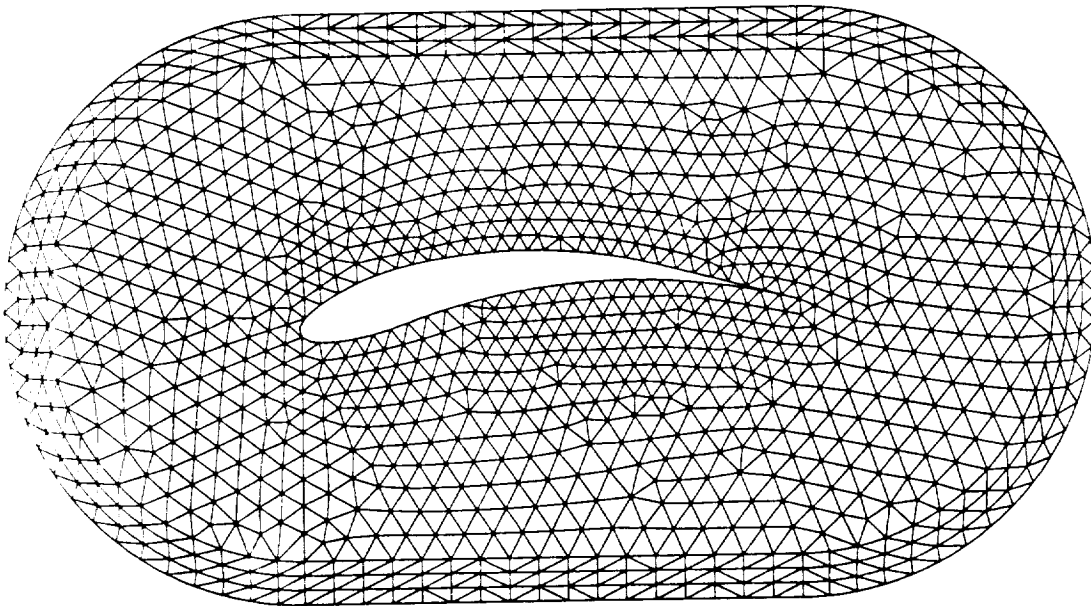
8

Figure 5: Mesh for Airfoil : Linear

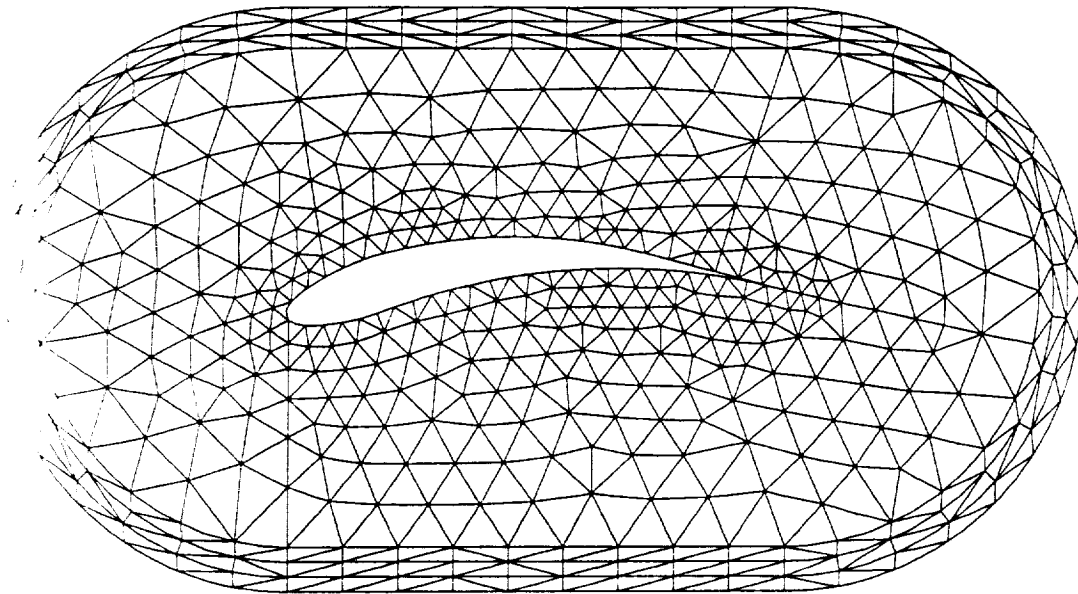Figure 6: Mesh for Airfoil : Parabolic

Figure 7: Mesh for Airfoil : Cubic

some modification to the cylinderical wave. Being able to efficiently discretize large regions is desirable since it is clear from the results for the airfoil that the artificial absorber must be placed far away from the scatterer. Actually, one could consider the transcendental Hankel function to be of exact accuracy limited only by numerical considerations. This is a feature that polynomial basis functions do not possess since they do not themselves solve the wave equation.

V. Conclusions

Although much more testing must be done with both the placement of the artificial absorber and the use of higher order and complex approximation functions, it is clear that this type of formulation holds promise for the accurate analysis of large scatterers. While many formulations are specific to a certain problem and do not allow for growth and modification, the above formulation and the software developed provide a flexible tool for improving the current state of FEM for the analysis of large electromagnetic scattering problems.

References

[1] Mei, K. K., "Unimoment Method of Solving Antenna and Scattering Problems," IEEE Transactions on Antennas and Propagation, AP-22, 760-766, 1974

[2] A. Bayliss, M. Gunzburger and E. Turkel, "Absorbing Boundary Conditions for the Numerical Solution of Elliptic Equations in Exterior Regions," SIAM J. Appl. Math., vol. 42, pp 430-451, April 1982.

[3] Jin and Volakis

[4] Jian-Ming Jin, John L. Volakis, and Valdis V. Liepa, "An Engineer's Approach for Terminating Finite Element Meshes in Scattering Analysis"

[5] Omar M. Ramahi and Raj Mittra, "Finite-Element Analysis of Dielectric Scatterers Using the Absorbing Boundary Condition," IEEE Transactions on Magnetics, Vol. 25, No. 4, pp 3043-3045, July 1989.

[6] Bayliss, A.,M. Gunzburger, and E. Turkel, "Boundary Conditions for the Numerical Solution of Elliptic Equations in Exterior Regions," SIAM J. Appl. Math., 42, 430-451, 1982

[7] Andrew F. Peterson and Richard J. Baca, "Error in the Finite Element Discretization of the Scalar Helmholtz Equation Over Electrically Large Regions," IEEE Microwave and Guided Wave Letters, Vol.1 No. 8, pp 219-222 August 1991.